Impact of urbanization and steel mill emissions on elemental composition of street dust and corresponding particle characterization

Klemen Teran[a],[*], Gorazd Žibret[a], Mattia Fanetti[b]

[a] *Geological Survey of Slovenia, Dimičeva 14, SI-1000 Ljubljana, Slovenia*
[b] *Materials Research Laboratory, University of Nova Gorica, Vipavska 11c, SI-5270 Ajdovščina, Slovenia*

GRAPHICAL ABSTRACT
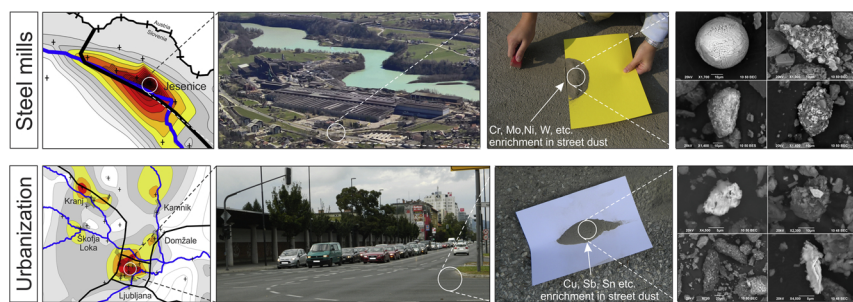
ARTICLE INFO

ABSTRACT

Street Dust (SD) acts as a sink and source of atmospheric particles containing Potentially Toxic Elements (PTEs) and can pose a possible pathway of PTEs to human bodies. Comprehensive SD study, where 249 samples were collected from rural, urban and industrialized areas aimed to increase the understanding between sedimentation of atmospheric dust derived from anthropogenic activities and elemental composition of SD. Elemental composition for 53 elements (ICP-MS, aqua regia digestion) was determined on fraction < 0.063 mm. Significantly increased levels of Sn-Cu-Sb-Bi-Ag-Ba-Mo-Pt-Pb and other elements have been detected in urban environments, compared to the rural ones. SEM/EDS investigation identified that main carriers of Ba, Cu and Sn are most likely particles derived from non-exhaust traffic emissions. Areas around steel mills show a strong enrichment with Cr, Mo, Ni and W, which exponentially decreases with the increased distance from the plant, reaching corresponding urban background 15 and 20 km from the source. SEM/EDS inspection identified spherical and melted irregular particles as the main carriers of the above-mentioned elements. City managers shall adapt measures to reduce amount of vehicular traffic and quantity of deposited SD on the public surfaces and encourage green city planning, while industrial emitters are encouraged to reduce their dust emissions.

1. Introduction

Urban areas and the rapid progress of industrialization are leading to serious air pollution. In Europe, more than two-thirds of the total population lives in cities. Despite efforts to maintain healthy urban environment, population growth and industrialization in some cities have led to air pollution that reaches levels that threaten human health, while emissions of CO_2 and other chemicals influence on climate (Cetin and Sevik, 2016) It is vital that urban spaces are planned according to the concept of sustainable urbanization, with the understanding of

[*] Corresponding author.
E-mail addresses: klemen.teran@geo-zs.si (K. Teran), gorazd.zibret@geo-zs.si (G. Žibret), mattia.fanetti@ung.si (M. Fanetti).

ecological planning, to enable environmentally sensitive urban development (Sevik et al., 2019). A number of green infrastructure solutions have been introduced to the open areas of different qualities within the city as a whole to improve quality of life (Turkyilmaz et al., 2018).

Particulate matter is hazardous material which strongly influence on human health within urbanized areas. Emissions form anthropogenic activities, especially from traffic, industry and fuel combustion overwhelm emissions from natural sources in urban areas (Hama et al., 2018). Anthropogenic airborne particles, especially those generated during combustion and other high temperature processes, are usually much smaller, have different morphology and have more complex elemental composition with higher levels of Potentially Toxic Elements (PTE) compared to the natural ones (Miler and Gosar, 2013). Their inhalation, ingestion or dermal contact represent a risk for human health, not only because of their physical properties, but also because PTEs in particles can be dissolved in body fluids and can trigger toxic effects in tissues and organs (Mbengue et al., 2015).

Suspended solid particles deposited on flat hard artificial surfaces, such as asphalt or concrete roads and pavements, contribute to the sediment called street dust (SD). SD is heterogeneous mixture of deposited atmospheric dust, particles formed during onroad processes, plant remnants, construction material debris and geogenic particles eroded from soils and rocks (Gunawardana et al., 2012). SD received a lot of scientific attention after it has been identified as an important sink for particles dispersed in atmosphere and major collector of PTEs in urban environments (Rasmussen et al., 2001). Furthermore, SD particle resuspension is one of the strongest contributors to the airborne particulate matter. Its share can reach up to 60% in urban environments (Padoan and Amato, 2018). Pant et al. (2015) discovered a statistically significant correlation between elemental composition of bulk SD (particle size < 2 mm) and PM_{10} particles sampled over the road. Specific PTEs in SD are found to be highly bioavailable (Mbengue et al., 2015) when ingested or inhaled, while others can be easily dissolved by rainwater, so the runoff water from urbanized areas can be highly toxic to aquatic organisms (McQueen et al., 2010). Therefore, contaminated SD could pose a threat to human health and to the environment.

Consistent regional study of SD elemental composition in diverse natural and anthropogenic environments, including urban as well as relatively remote, sparsely populated countryside environments, are missing from world's scientific literature. Such studies can serve as an

important source of scientific information to define proper sampling, analytical and data interpretation protocols to establish SD as a proxy for atmospheric contamination with particulate matter. Identified regional anomalies and trends can therefore be used as an input for better local and regional planning. The objective of this study is to conduct a comprehensive SD sampling campaign, including urban and rural environments, and to perform SEM/EDS observation on particle level, to determine potential causes of larger anomalies. The results of this study underline the importance of ecological approaches in landscape design studies in sustainable cities, while they provide valuable insights, not only for the experts in the field of atmospheric dust, but also to policy makers, urban planners and landscape architects.

2. Materials and methods

2.1. Description of the study area

The study area covered almost the whole territory of Slovenia, spanning from 13.38 °E to 16.62 °E, and 45.42 °N to 46.88 °N (Fig. 1). Slovenia has a diverse climate, topography, geological composition and variably urbanized and industrialized areas. Three different climate types exist in Slovenia. Most of the country has a warm-summer humid continental climate (Dfb), SW part experiences hot-summer Mediterranean climate (Csa) and a tundra climate (ET) is present in the mountains in N part. Predominant direction of humid air masses from SW and orographic barriers in the W part of the country results in high precipitation rates in the W Slovenia, reaching up to 3200 mm per year, while in E area average annual precipitation is 900 mm. Although wind directions are very variable and strongly dependent on local morphology and other circumstances, westerly wind generally prevails over the study area.

Three steel mills are located in the study area and one is situated in its immediate vicinity (Fig. 1). Jesenice and Ravne steel mills use Electric Arc Furnace (EAF) which is feed with scrap metal to produce stainless-steel, with a cumulative annual production of 450,000 t. EAF steel mill in Štore is producing forging bars and cast steel from scrap metal, with an annual production of 140,000 t. Integrated steel mill in Trieste (Italy) located only 4 km from Slovenian border is comprised of coke plant, iron ore sintering plant and of two blast furnaces with an annual production of approximately 450,000 t of pig iron.
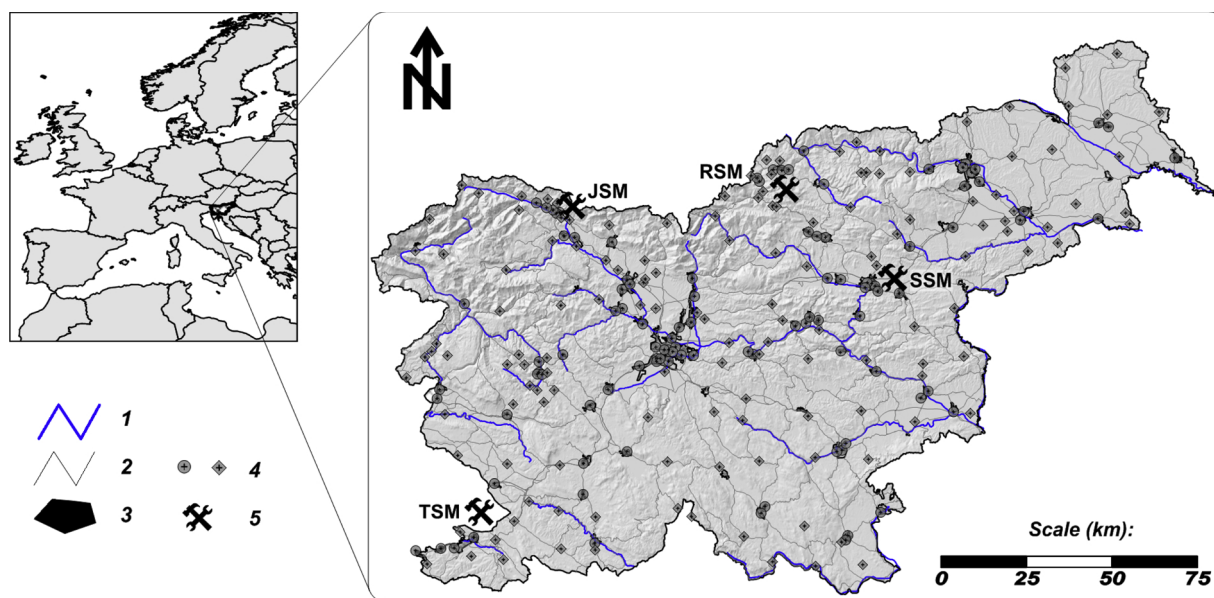
Fig. 1. The location of study area.
Key of symbols: 1 - rivers; 2 - major roads; 3 - towns; 4 – SD sampling locations; circles - towns and diamonds - countryside; 5 - larger steel mills; JSM - Jesenice steel mill; RSM – Ravne steel mill; SSM - Štore steel mill; TSM - Trieste steel mill (Italy).

2.2. Sampling and sample preparation procedure

SD sampling was carried out during summer period of 2016 on 249 sampling locations spread over rural, urban and industrialized areas (Fig. 1). Sampling point locations and corresponding levels of for Cr, Cu, Mo, Ni, Sb and Sn are listed on Table SM1 in Supplementary material.

SD was collected from pores in asphalt or concrete surfaces using plastic brush and was pre-processed according to the procedure described in Žibret et al. (2013). Field duplicates were taken and analyzed from 23 sampling locations but are not discussed in this paper. Samples with particle size < 0.063 mm were analyzed at Bureau Veritas Upstream Minerals in Vancouver, Canada using ICP-MS following the modified Aqua Regia digestion method. Their extended ultratrace ICP-MS method, where 0.5 g of sample was digested in mixture of HNO_3, HCl and H_2O, with ratio 1:1:1 at temperature 95 °C, provided analysis for 53 major, minor and trace elements.

2.3. Quality control

36 Certified Reference Materials (CRM) were randomly added to the analytical batch to monitor quality control of the chemical analyses. Analyzed CRMs were BCR-723 (street dust, n = 4), BCR-176R (fly ash, n = 1), BCR-142R (light sandy soil, n = 1), ERM-CC141 (loam soil, n = 1), BCR-320R (channel sediment, n = 1), STD DS10 (internal laboratory standard, n = 14), and OREAS 25a (soil blank, n = 14). Additionally, 42 duplicates of randomly selected samples were added to the analytical batch. List of duplicates with corresponding results of chemical analyses is listed on Table SM2 in Supplementary material.

Recovery rate (%R, Eq. (1)) and Average Relative Percent Difference (ARPD, Eq. (2)) were calculated and assessed.

$$\%R = \frac{100}{n} \cdot \sum_{i=1}^{n} \left[1 + \frac{CM_i - CS_i}{CS_i} \right] \tag{1}$$

CM_i - average measured level of element i in analyzed CRM; CS_i - certified level of element i in CRM.

$$ARPD = \frac{200}{n} \cdot \sum_{i=1}^{n} \frac{|CM_i - CR_i|}{CM_i + CR_i} \tag{2}$$

CM_i - measured level of element i in the sample; CR_i - measured level of element i in sample analysis repetition.

2.4. Data processing

Elements with more than one third of measurements below the detection limit (Hf, In, Pd, Re, S, Se and Ta) were not included in further data processing. For other elements, all values under detection limit were replaced by the value of 50% of the corresponding detection limit value. Where double analysis was made for precision test, the actual level was assumed to be an average value of both analyses. Nonparametric statistics (median, minimum, maximum and percentile distribution) was calculated first. Nonparametric Mann-Whitney U test was used to test differences in elemental distribution between samples taken in urban and countryside environments. Nonparametric method was selected instead of parametric Student t-test because obtained results were not normally distributed, did not have homogeneity of variance and contained outliers. Samples were divided into urban (samples from settlements with more than 5000 inhabitants – 105 samples) and countryside (144 samples) group.

Enrichment Factors (EF) for SD (Eq. (3)) were calculated according to topsoil background elemental levels (Gosar et al., 2019). Aluminum was used as normalizing element, because its distribution in soil is not affected by anthropogenic activities. EF below 2 suggests no significant enrichment while EF above 2 indicates moderate, 5–20 significant, 20–40 high and EF above 40 extreme enrichment (Barbieri, 2016).

$$EF = \frac{\frac{C_{x\,(SD)}}{C_{Al\,(SD)}}}{\frac{C_{x\,(soil)}}{C_{Al\,(soil)}}} = \frac{C_{x\,(SD)} * C_{Al\,(soil)}}{C_{x\,(soil)} * C_{Al\,(SD)}} \tag{3}$$

$C_{x\,(SD)}$ - median of selected chemical element in SD sample; $C_{Al\,(SD)}$ - Al level (reference element) in SD sample; $C_{x\,(soil)}$ - median level of selected chemical element in topsoil sample; $C_{Al\,(soil)}$ - Al level measured in topsoil.

2.5. SEM/EDS

Morphological and semi-quantitative X-ray microanalyses of individual solid particles with diameter < 0.063 mm extracted from SD were performed on unpolished samples mounted on a double-sided carbon tape and sputter coated with a thin carbon layer to improve conductivity. The SEM/EDS analysis was carried out in a high vacuum using a JEOL JSM 6490 L V SEM coupled with an Oxford INCA PentaFETx3 Si(Li) detector and INCA Energy 350 processing software at 20 kV accelerating voltage and 10 mm working distance. PTE bearing particles were identified in Back-Scattered Electron (BSE) mode, while EDS analysis was performed to identify semi-quantitative elemental composition for metal bearing particles. EDS spectra acquisition time was set to 90 s.

3. Results

Quality control results (Table 1) show that %R for most of the analyzed elements ranged between 85 and 115%. Elements with %R below 85 % (Au and Ba) as well as elements with %R above 115 % (Be) were excluded form further statistical analyses while other were retained. Precision parameter ARPD for most elements was below 12%, except for the W (23%), Bi (25%), Te (38%), Pt (40%), Ag (47%), Hg (49%), Be (66%) and Au (90 %). Poor ARPD values indicate inhomogeneous distribution of specific elements within SD. This is either a consequence of insufficient homogenization or metal clustering effect in the sample, to which several listed elements are prone to.

Non-parametric statistics (Table 1) show that Ca and Mg are predominant among all analyzed elements with medians above 1%. Median levels of Fe and Al in collected SD exceeded 0.1%, while medians for K, P, Na, Mn, Ti and Zn exceed 0.01%.

Extreme EF (Fig. 2) have been calculated for Ca (136) and Sn (51) in urban environments and for Ca (125) and Mg (42) at countryside. High EF were calculated for Mg (37) and Sr for urban environments while countryside shows high EF for Sn (21) and Sr (21). Significantly enriched elements in both environments were Cu, Mo, Na, Sb, Ti and Zn, while Ag, Bi and Pb are significantly enriched only in urban environments.

Mann-Whitney U test confirmed that the distribution of SD elemental levels in countryside and urban environments differs for 24 elements (Fig. 3). Urban environments show higher levels of Sn, Cu, Sb, Bi, Ag, Mo, Pt, Pb, Cr, Zn, W, Ni, Hg, Cd, Fe, Ti, Sr, Nb and Ca, while Rb, Th, K and Mg are depleted in urban environments. Spatial distributions of Sn, Cu and Sb, which show the biggest differences between their distribution, are presented on dot distribution map, accompanied by map of population density in Fig. 4(a–d).

Spatial distribution of elemental levels in SD shows that anomalies of Co, Cr, Fe, Mo, Nb, Ni and W exist around Jesenice steel plant, and anomalies of As, Cd, Cr, Mn, Mo, Ni, U, V, W and Zn around Ravne steel plant. Fig. 5(A–D) shows a strong correlation between centers of anomalies of Cr, Mo, Ni and W and the locations of steel mills at Jesenice (JSM) and at Ravne (RSM). Anomaly marked with SSM represents slightly elevated Cr, Mo and Ni levels around Štore steel mill. The geographic distribution of Cr, Mo, Ni and W also shows extensive anomaly spreading across W-SW part of Slovenia (K-F) and near Trieste, where integrated steel mill is situated (TSM). Above average Cr, Mo Ni and W levels were additionally detected in Ljubljana and Maribor

Table 1

Percentile distribution of elements in SD in Slovenian towns (N = 105) and countryside (N = 144).

EL	UN	DL	ARPD [%]	%R	Countryside[a]	Urban environment[a]	SLO
Ag	mg/kg	0.002	47	99	0.011 –0.032 - 0.051 - 0.12 - 7.2	0.024 – 0.096 – 0.26 – 0.59 – 7.4	0.062
Al	%	0.01	3	106	0.18 - 0.38 - 0.52 - 0.73 - 2.0	0.22 - 0.38 - 0.52 - 0.62 - 1.6	1.8
As	mg/kg	0.1	10	100	1.3 - 3.1 - 4.2 - 5.4 - 17	1.7 - 3.3 - 4.1 - 4.9 - 20	11
Au	mg/kg	0.0002	90	78	< DL – 0.00075 – 0.0018 – 0.0042 – 1.8	0.0007 – 0.0042 – 0.015 – 0.081 – 1.9	0.0017
Ba	mg/kg	0.5	4	77	14 - 39 - 54 - 81 - 300	29 - 62 - 92 - 130 - 1900	75
Be	mg/kg	0.1	66	119	< DL - 0.20 - 0.30 - 0.40 - 1.1	< DL - 0.20 - 0.30 - 0.35 - 1.3	0.90
Bi	mg/kg	0.02	25	111	0.080 - 0.21 - 0.38 - 0.59 - 4.2	0.23 - 0.56 - 0.77 - 1.0 - 6.5	0.33
Ca	%	0.01	3	105	3.4 - 12 - 16 - 19 - 27	3.9 - 14 - 17 - 20 - 27	0.44
Cd	mg/kg	0.01	9	106	0.14 - 0.33 - 0.48 - 0.70 - 29	0.25 - 0.46 - 0.60 - 0.84 - 75	0.47
Ce	mg/kg	0.1	5	101	4.8 - 8.4 - 11 - 15 - 37	4.0 - 8.5 - 11 - 13 - 26	38
Co	mg/kg	0.1	5	98	0.80 - 3.2 - 4.5 - 6.9 - 22	1.7 - 4.0 - 5.0 - 6.4 - 26	14
Cr	mg/kg	0.5	5	93	7.5 - 20 - 29 - 43 - 330	14 - 33 - 45 - 68 - 1800	34
Cs	mg/kg	0.02	4	100	0.24 - 0.47 - 0.57 - 0.69 - 4.9	0.27 - 0.43 - 0.54 - 0.62 - 1.8	1.4
Cu	mg/kg	0.01	5	101	7.8 - 23 - 37 - 60 - 420	19 - 57 - 75 - 120 - 340	20
Fe	%	0.01	2	99	0.30 - 0.88 - 1.2 - 1.6 - 3.6	0.62 - 1.1 - 1.4 - 1.7 - 5.3	2.9
Ga	mg/kg	0.1	7	105	0.40 - 1.0 - 1.4 - 2.1 - 6.2	0.60 - 1.1 - 1.3 - 1.8 - 5.2	5.2
Hg	mg/kg	0.005	49	87	0.010 -0.027 - 0.048 - 0.11 - 9.9	< DL - 0.044 - 0.080 - 0.19 - 70	0.11
K	%	0.01	3	107	0.030 - 0.050 - 0.070 - 0.088 - 0.32	0.030 - 0.050 - 0.060 - 0.080 - 0.37	0.11
La	mg/kg	0.5	5	103	2.4 - 4.1 - 5.7 - 7.3 - 20	2.2 - 4.4 - 5.6 - 7.4 - 13	17
Li	mg/kg	0.1	6	107	2.0 - 4.0 - 5.7 - 8.1 - 19	2.2 - 4.2 - 5.5 - 6.8 - 18	19
Mg	%	0.01	2	102	0.53 - 3.7 - 5.6 - 6.6 - 9.6	0.66 - 3.9 - 4.9 - 5.8 - 8.6	0.46
Mn	mg/kg	1	2	99	120 - 250 - 330 - 460 - 2500	130 - 270 - 330 - 450 - 3600	790
Mo	mg/kg	0.01	7	100	0.46 - 1.1 - 1.8 - 2.8 - 23	0.57 - 2.3 - 3.1 - 4.8 - 190	0.72
Na	%	0.001	6	106	0.0070 - 0.017 - 0.021 - 0.029 - 0.58	0.0080 - 0.017 - 0.020 - 0.029 - 0.73	0.0070
Nb	mg/kg	0.02	7	92	0.090 - 0.25 - 0.34 - 0.60 - 4.3	0.16 - 0.31 - 0.39 - 0.55 - 4.6	0.60
Ni	mg/kg	0.1	6	100	4.7 - 13 - 19 - 27 - 220	9.4 - 18 - 24 - 33 - 1300	29
P	%	0.001	4	102	0.014 - 0.031 - 0.046 - 0.063 - 0.17	0.021 - 0.036 - 0.044 - 0.061 - 0.26	0.054
Pb	mg/kg	0.01	5	107	7.2 - 16 - 24 - 40 - 3900	15 - 30 - 54 - 90 - 3800	34
Pt	mg/kg	0.002	40	101	< DL – 0.002 – 0.004 – 0.007 – 0.055	< DL – 0.0055 – 0.010 – 0.014 – 0.079	–
Rb	mg/kg	0.1	4	105	2.5 - 4.5 - 6.3 - 8.1 - 29	2.2 - 4.0 - 5.2 - 6.8 - 21	18
Sb	mg/kg	0.02	5	94	0.23 - 0.77 - 1.4 - 2.3 - 40	0.45 - 2.2 - 3.0 - 4.4 - 17	0.53
Sc	mg/kg	0.1	8	104	0.60 - 1.3 - 1.7 - 2.2 - 4.5	0.70 - 1.4 - 1.8 - 2.2 - 7.1	3.9
Sn	mg/kg	0.1	12	110	1.3 - 3.9 - 6.8 - 11 - 54	3.3 - 11 - 16 - 22 - 110	1.1
Sr	mg/kg	0.5	3	112	27 - 56 - 84 - 130 - 420	34 - 71 - 98 - 150 - 340	14
Te	mg/kg	0.02	38	113	< DL - < DL - 0.030 - 0.040 - 0.080	< DL - < DL - 0.020 - 0.038 - 0.23	0.040
Th	mg/kg	0.1	5	104	0.30 - 0.80 - 1.1 - 1.6 - 5.1	0.40 - 0.70 - 0.90 - 1.2 - 2.6	4.1
Ti	%	0.001	3	99	0.0020 - 0.0070 - 0.011 - 0.027 - 0.26	0.0060 - 0.010 - 0.014 - 0.026 - 0.26	0.0060
Tl	mg/kg	0.02	5	96	0.030 - 0.060 - 0.080 - 0.11 - 0.55	0.030 - 0.060 - 0.070 - 0.090 - 0.93	0.23
U	mg/kg	0.1	2	110	0.40 - 0.70 - 0.90 - 1.3 - 2.3	0.30 - 0.70 - 1.0 - 1.3 - 2.4	1.0
V	mg/kg	2	3	103	9.0 - 16 - 21 - 28 - 79	9.0 - 17 - 21 - 27 - 120	40
W	mg/kg	0.1	23	97	< DL - 0.20 - 0.33 - 0.75 - 6.1	< DL - 0.40 - 0.60 - 1.1 - 58	–
Y	mg/kg	0.01	4	106	1.8 - 3.9 - 4.8 - 5.9 - 21	2.3 - 3.9 - 4.6 - 5.7 - 10	11
Zn	mg/kg	0.1	3	99	32 - 98 - 140 - 250 - 3700	81 - 190 - 270 - 360 - 11000	72
Zr	mg/kg	0.1	10	106	< DL - 0.50 - 0.70 - 1.1 - 4.2	< DL - 0.50 - 0.80 - 1.1 - 13	1.8

[a] elemental levels are presented as: minimum - 25th percentile - median - 75th percentile and maximum. EL - element; UN - unit; DL - detection limit; < DL - below detection limit; ARPD - precision control, average relative percent difference; %R - accuracy control, average recovery rate; countryside - percentile distribution of elemental levels in SD in countryside; urban environment - percentile distribution of elemental levels in SD in towns; SLO-median elemental levels for Slovenian soil (Gosar et al., 2019), aqua regia digestion methods.

urbanized areas. Scaling of SD elemental levels with the distance from Ravne and Jesenice steel mills (Fig. 6) shows exponential decrease of Cr, Mo, Ni and W levels in SD with increasing distance from the steel making plant. Coefficients of determination (R^2) up to 0.67 show good fitting of trends with the measured levels.

SEM/EDS inspection of SD samples was focused on identifying characteristic particles containing Cu, Sb and Sn in SD from urbanized areas, and carriers of Cr, Mo, Ni and W in SD around steel mills. To detect whether similar characteristic particles, carriers of the above mentioned elements, are also present in particles in non-contaminated areas, similar SEM/EDS observations were also conducted on SD samples collected from countryside.

The most commonly observed objects in SD samples collected in urbanized areas are particle agglomerations with diameters from a few μm to 60 μm. The agglomerations frequently contain PTE bearing particles with diameters between 0.5 and 10 μm. As an example, the agglomerate on Fig. 7/1 contains Fe-Mn-O particle (bright on the electron image) with traces of Al, Cu, S, Si, Sn and Zn (SM7/1). Other PTE bearing objects are the organic thread-like particles, which are composed mainly of C, Ca, Fe, S and O and contain traces of Al, Ba, Cu, Cl,

Mg and Ti (Fig. 7/2 and SM7/2). Particle's short axis' diameter is around 10 μm and long axis up to 100 μm. Several other smaller particles of various compositions are adhered on their surface. Some PTE bearing particles are not observed agglomerated but isolated. An example is Ba-S-Si-O particle with diameter around 10 μm (Fig. 7/3), containing also Al, Ca, Cu, Fe, Na, Ti, Zn etc. (SM7/3). Spherical particles in urban SD commonly contain ferrous oxides and their morphology is similar to the ones detected around steel mills (see Fig. 8a and b, described in the next paragraph). However, they differ from those particles in elemental composition, as they seldom contain trace elements, which are very abundant in spherical particles found around steel mills. A second type of spherical particles are soot particles composed, for instance, of Al, Ca, Fe, Mg, Si and O with traces of K, Na and Ti (Fig. 7/4 and SM7/4). Another observed species are elongated striated shavings of different alloys. One example is shown in Fig. 7/5. Such particles can be longer than 100 μm, and their thickness is in the range of 2 to 20 μm. They are composed of pure Fe or Fe and Mn, with traces of Al, Ca, Cu, O and Si (SM7/5). Finally, another particle type detected in urban SD are mineral microfibers or Man-Made Vitreous Fibers (MMVF) with diameters of around 10 μm and length reaching
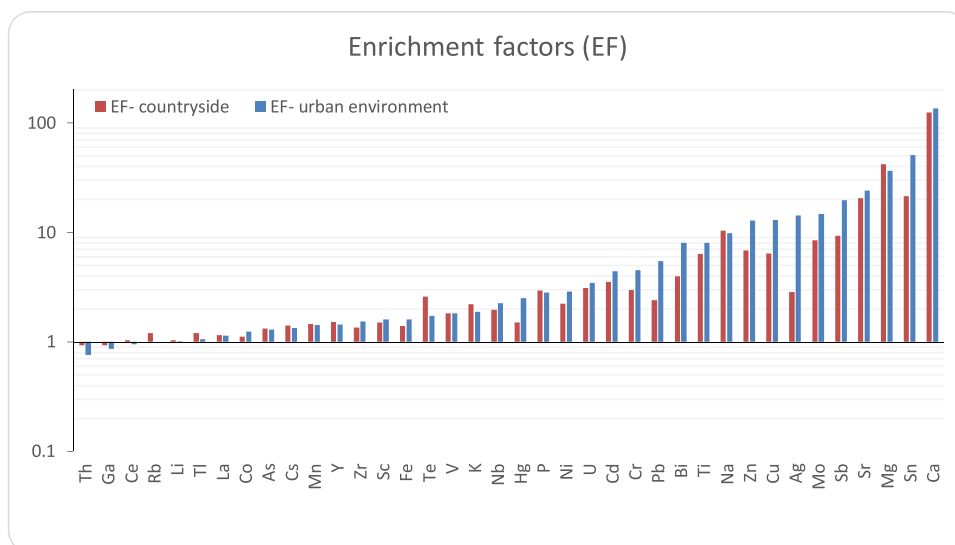
Fig. 2. Enrichment factors for SD.
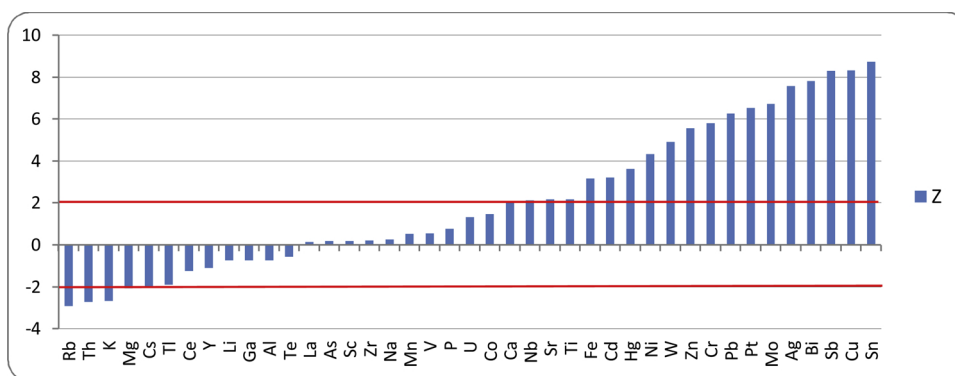
Fig. 3. Mann-Whitney U test results for detection of difference between countryside (105 samples) and urban environment (144 samples). Z – Wilcoxon Z; values above 2 or below -2 show statistically significant difference (with p < 0.05).

100 µm (Fig. 7/6). MMVF matrix was composed of Al, Ca, Mg, Si and O, with traces of K, Mn, Na and Ti, while micrometer inclusions contain increased levels of Fe and P (SM7/6 and SM7/6-a).

SEM/EDS particle inspection of SD collected around the steel mills identified two categories of particles as the main carriers of Cr, Mo Ni and W: spherical and irregular.

Spherical particles have diameters from 2 to 60 µm. They can be divided into hollow spherical particles (Fig. 8a and b) which prevail over filled spherical ones. Hollow spheres are most commonly characterized by porous dendritic surface morphology, frequently with visible aperture (Fig. 8a). EDS spectra (SM8a and SM8b) indicates that they are composed mainly of Fe, Cr, Ni and O with traces of Al, Ca, Cu, Mg, K, Mn, Mo, Ni, Si and Zn. Some particles have a simple elemental composition as is Fe-O, Fe-Cr-O or Fe-Cr-Ni-O, while others contain the whole array of listed elements. Filled spheres contain mainly Fe and O with traces of Al, Ca, Cr, Mg and Si.

Irregular particles have length of the longer axis between 5 and 40 µm. They show various particle morphologies, sometimes with relatively plain, smooth surfaces (Fig. 8c and f) and sometimes more complex surfaces with bubble-shaped perturbances and cavities. (Fig. 8d and e) The main constituents of such particles are Fe, Ca, Cr and O with traces of Al, Cu, Mg, Mn, Mo, Ni, Si, V, W and Zn (SM8c–SM8f).

4. Discussion

The most distinctive anomalies detected in this study are high-magnitude but low spatial extension anomalies of Cr, Mo Ni and W

spreading around active steel mills. Maximum levels of Cr, Mo, Ni and W were amounted to 1800, 190, 1300 and 58 mg/kg respectively, exceeding background levels for 40, 61, 54 and 97 times respectively. Similar shape of their exponential regression line indicates the same source and transport mechanisms. A 10-fold decrease of elemental levels in the first 5 km indicates particle sedimentation near the emission source, where especially larger particles are quickly deposited, while background elemental levels are reached approximately between 15 and 20 km from the steel making plant (Fig. 6). Detected influence area around steel mill in this study is smaller as in the case of Ledoux et al. (2017), who reported an area of influence for similar industrial areas to be 35 km. The most probable reason for that is a smaller quantity of steel produced in Slovenian steel mills and the orographic barriers, which limit the dispersion of particles by wind. Increased levels of Cr, Fe and Ni in topsoil of Jesenice area have already been reported by Šajn (1998), and increased levels of Cr, Mo, Ni and W in attic dust and topsoil around Ravne by Šajn (2006). Both studies identified steel mills as the main source for these anomalies. However, aforementioned studies detected accumulative effects of steel production through time, while this study demonstrates recent state, as it was during the sampling campaign, indicating that present-day dust emissions still exists and can be reflected in SD composition.

Detected Cr, Mo, Ni and W anomalies in this study generally follow local topography, indicating that the main mechanism of dispersion is air transport of metal-bearing particles along river valleys. Observed Cr, Ni and W anomalies on Jesenice and Ravne have approximately the same extent, while Mo anomaly at Ravne is larger. This can be
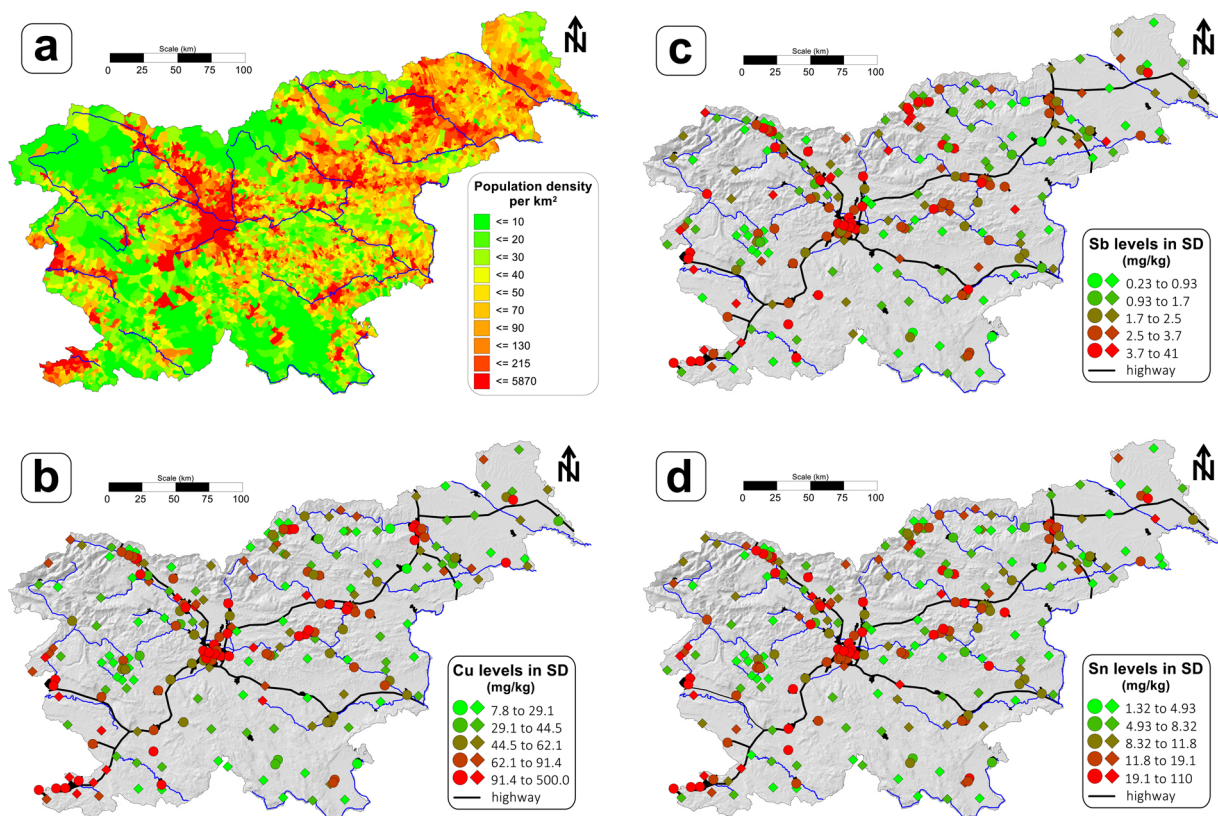
Fig. 4. Population density (a) and distribution of Sn, Sb, Cu in SD from towns (circles) and countryside (diamonds) (b–d).
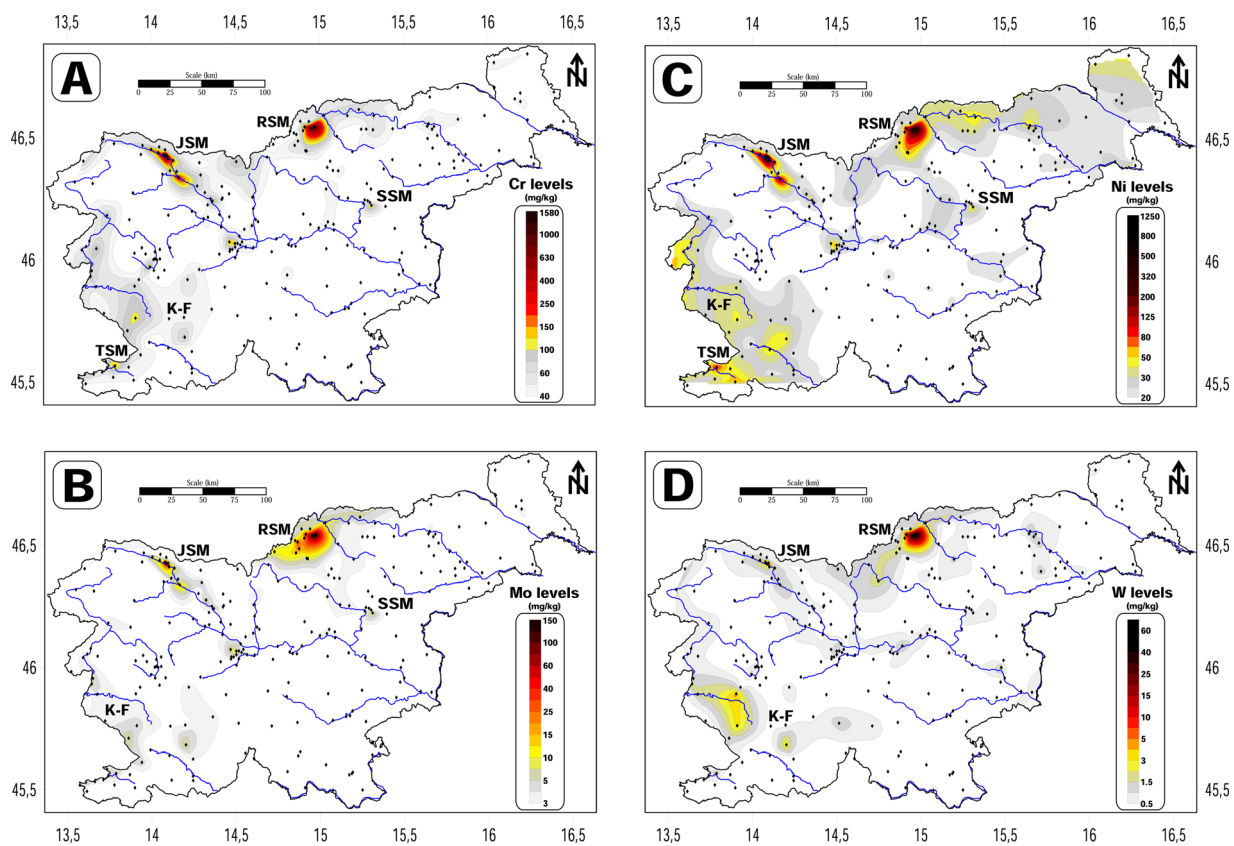
Fig. 5. The maps of detected anomalies in SD. A – map of Cr anomalies, B – map of Mo anomalies, C – map of Ni anomalies and D – map of W anomalies. Abbreviations on the maps: JSM – Jesenice steel mill, RSM – Ravne steel mill, SSM - Štore steel mill and TSM – Trieste steel mill. Anomalies marked with K-F corresponds to the occurrence of Paleogene flysch sediments and karstic residual soils.
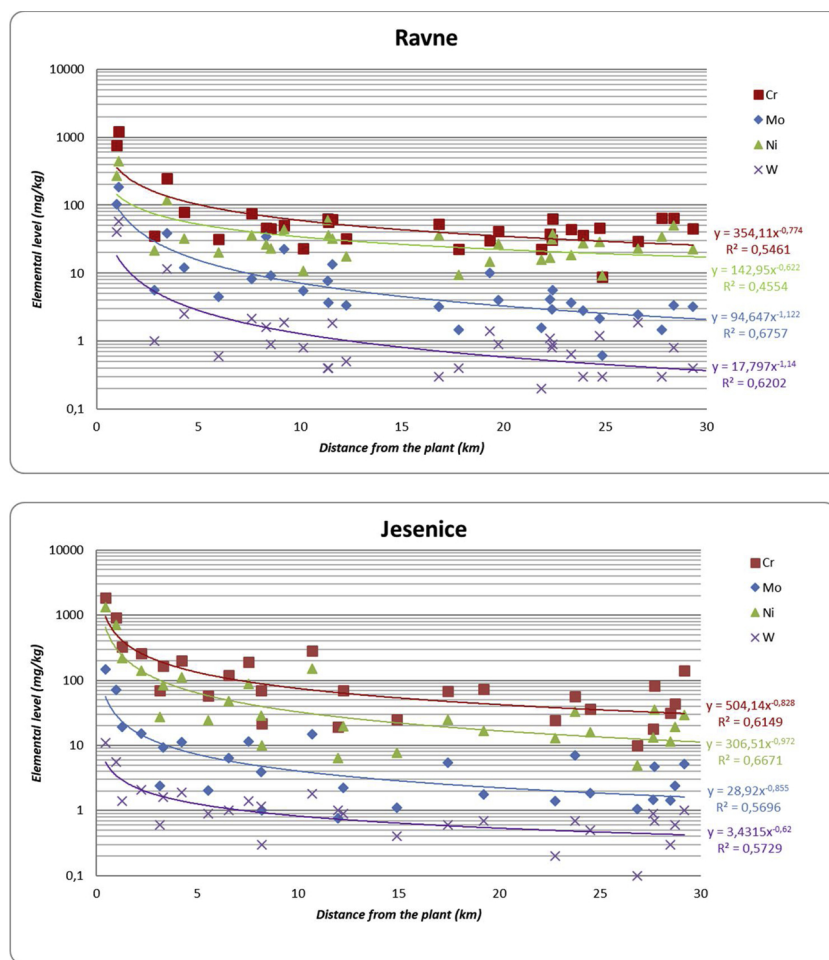
Fig. 6. Scaling of elemental levels in SD and distance from the two major steel mills Ravne and Jesenice and exponential trends of decreasing of elemental levels of Cr, Ni, Mo and W with the distance from steel mills.

explained by the fact that Ravne area can be influenced also by re-suspension of material from old Pb-Zn mining waste from the nearby Mežica mine, located 8 km upstream of Ravne (Miler and Gosar, 2019), because this mining waste can contain significant amounts of wulfenite ($PbMoO_4$).

Although Cr, Mo and Ni anomalies were also detected around Štore steel mill they are hardly notable. This can be attributed to the lower steel production, different processes involved and installation of new dust filters (Žibret, 2012). These results show that proper dust control measures in steel mills can decrease their impact to SD composition almost to the background levels. Area in the vicinity of Trieste integrated steel mill showed only slight anomaly of Cr and Mo levels in SD, despite of approximately 380 t of emitted atmospheric dust per year (Boscolo and Padoano, 2011), most probably due to the different processes applied in integrated steel mills which release particles enriched mainly with Al, Ca, Fe, Mn, Pb and Zn (Sylvestre et al., 2017).

Beside steel mill emissions, traffic and other industry in larger urbanized areas could also emit Cr, Mo, Ni and W enriched particles (Gaberšek and Gosar, 2018), but, as this study shows, these emissions are very low, compared to those from steel mills.

Electron microscopy revealed that PTE bearing particles identified in samples around steel mill significantly differ in morphology and elemental composition from PTE bearing particles deposited in urban or countryside environments. Spherical particles from the vicinity of steel mills contain, beside Fe, Ca and O, also significant amounts of Cr, Cu, Mn, Mo, Ni and Zn. In particular, Cr and Ni can represent even major constituents of such particles. Furthermore, irregular particles with bubble-shaped protuberances and cavities, commonly found in SD from

vicinity of steel mills, were not found in other environments. These particles also contain high levels of Cr, Mn, Mo, Ni and in some cases also V and W. Spherical particles and irregular particles with cavities and perturbances are characteristic for high temperature processes, while chemical composition corresponds to the steel alloying elements which additionally confirm steel mills as their source. Powell et al. (2002) found similar particles composed of Fe-V-Cr and Fe-Ca-La in house dust sampled in vicinity of steel mill, while steel mill emissions in other studies were characterized by Mo, Fe-Cr and Fe-Zn particles (Xie et al., 2009) and irregularly shaped Fe-oxides, Fe-alloys as well as spherical Fe-oxides and Fe-silicates, with various presence of Cr, Mn, Ni, Mo, V and W (Miler and Gosar, 2015).

SEM/EDS inspection also revealed difference in particulate matter emissions from EAF and integrated steel mills. SD collected in the vicinity of Trieste integrated steel mill contains mainly hollow spherical PTE bearing particles, while irregular particles either with plain or bubble shaped surface were absent. Spherical particles showed a simple elemental composition, in most cases composed of Fe and O, which is in contrast with spherical particles observed in SD around EAF steel mills containing large amounts of trace elements. That difference furthermore explains less pronounced Cr, Mo, Ni and W anomaly in vicinity of Trieste.

Extensive anomaly of Cr, Mo, Ni and W in western part of Slovenia is most likely a consequence of soil resuspension by strong wind or because of farming. Soils developed on flysch rocks and karstified limestones which outcrop on that area, differ from other soils and show strong enrichments with all listed elements (Zupančič et al., 2018).

The second well expressed anthropogenic impact to the SD
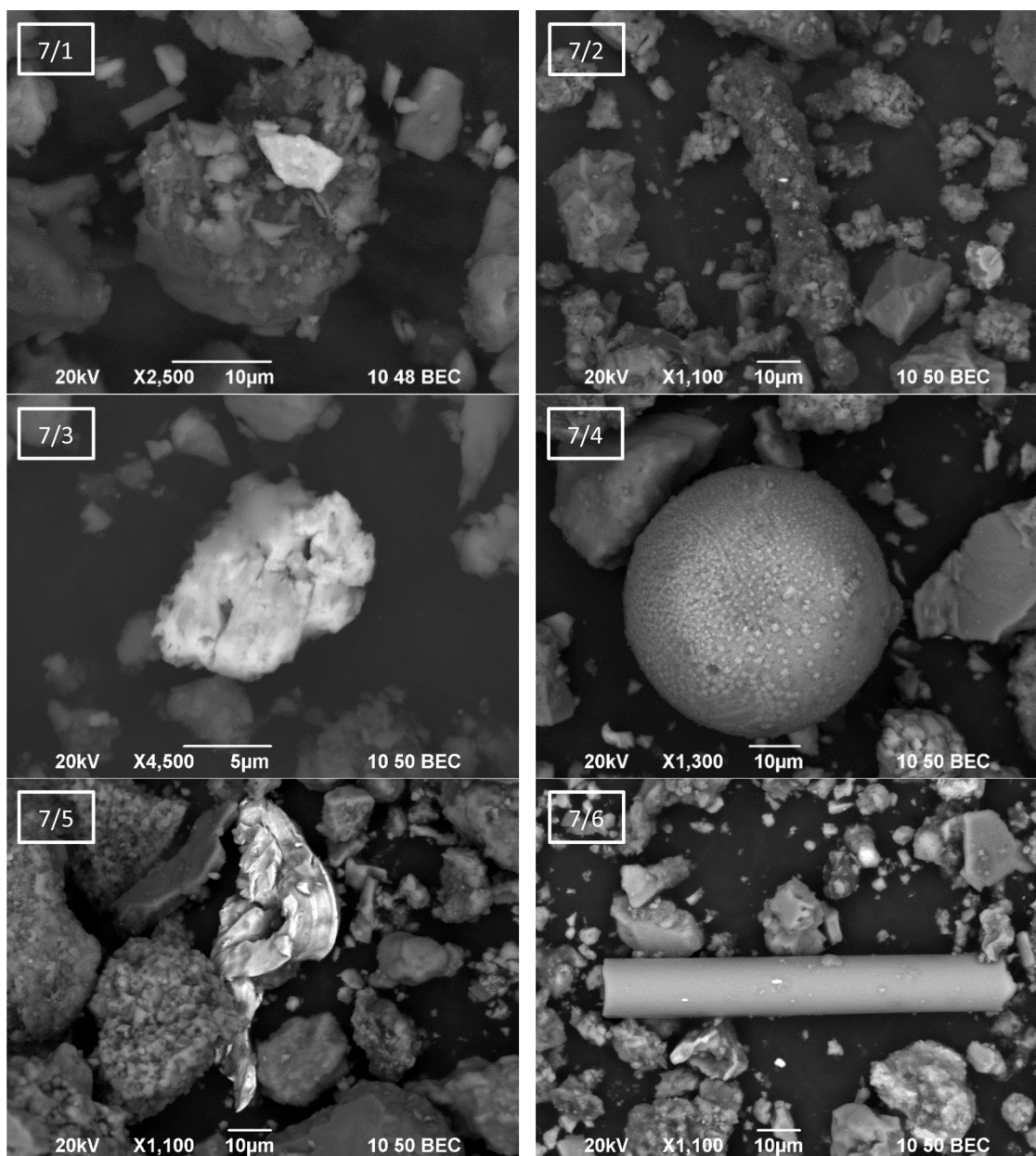
Fig. 7. SEM images of PTE carrying particles characteristic for urban environment. Micrographs were made in BSE mode.

composition corresponds to the impact of urbanization. Žibret (2018) characterized elemental association Ag–Bi–Ca–Cd–Mg–Mo–Pb–Zn in SD as a consequence of different processes, typical for urbanization. This is in the agreement with the results of this study, which added also Sn, Cu, Sb, Pt, Cr, W, Ni, Hg, Fe, Ti, Sr, Nb to this list.

Cu, Sb and Sn have the highest enrichments in urbanized areas compared to the countryside. Spatial distribution patterns for these elements show that the highest levels are clustered in urban centers (Ljubljana, Maribor, Celje, Kranj, etc.) as well as along river valleys and basins which have the highest population density, as well as also along Slovenian highway cross, indicating that traffic emissions might be one of the most important sources of urban particles (Fig. 4).

SEM/EDS inspection of SD collected in urban areas identified particle agglomerates, isolated irregular particles with plain surface and tile-like shape and organic thread-like particles as the main carriers of Ba, Cu and Sn. Their shape, size and elemental composition corresponds well with the particles identified during brake pad abrasion tests by Kukutschová et al. (2011), where particles larger than 1 μm were tile-

like shaped and were composed of Fe, Cu, Sn and Zn. The presence of Ba in such particles is mainly because Ba-sulfide is used as a filler in brake pads (Grigoratos and Martini, 2015). The presence of such particles in high quantities is probably the reason why high EFs for Cu, Sn and Zn were detected in urban environments.

Organic thread-like particles consist mainly of C, S and O and contain traces of Ba, Cu, Cl and Fe. Numerous smaller particles with various morphologies are adhered on their surface. This corresponds well with particles identified by Tian et al. (2017) who recognized such particles as tire wear products. Traffic non-exhaust sources are therefore the main source of observed particle agglomerates, isolated irregular particles and organic thread-like particles, abundant for SD in urban areas. It needs to be noted, that Sb levels in bulk SD are too low for SEM/EDS identification of carrier particles on such a scale. However, Sb is significantly enriched in SD compared to topsoil, it shows similar spatial distribution as Cu and Sn, and it is commonly one of the major components in brake pads (Thorpe and Harrison, 2008). Therefore, we can conclude that the strong enrichment of Sb in urban
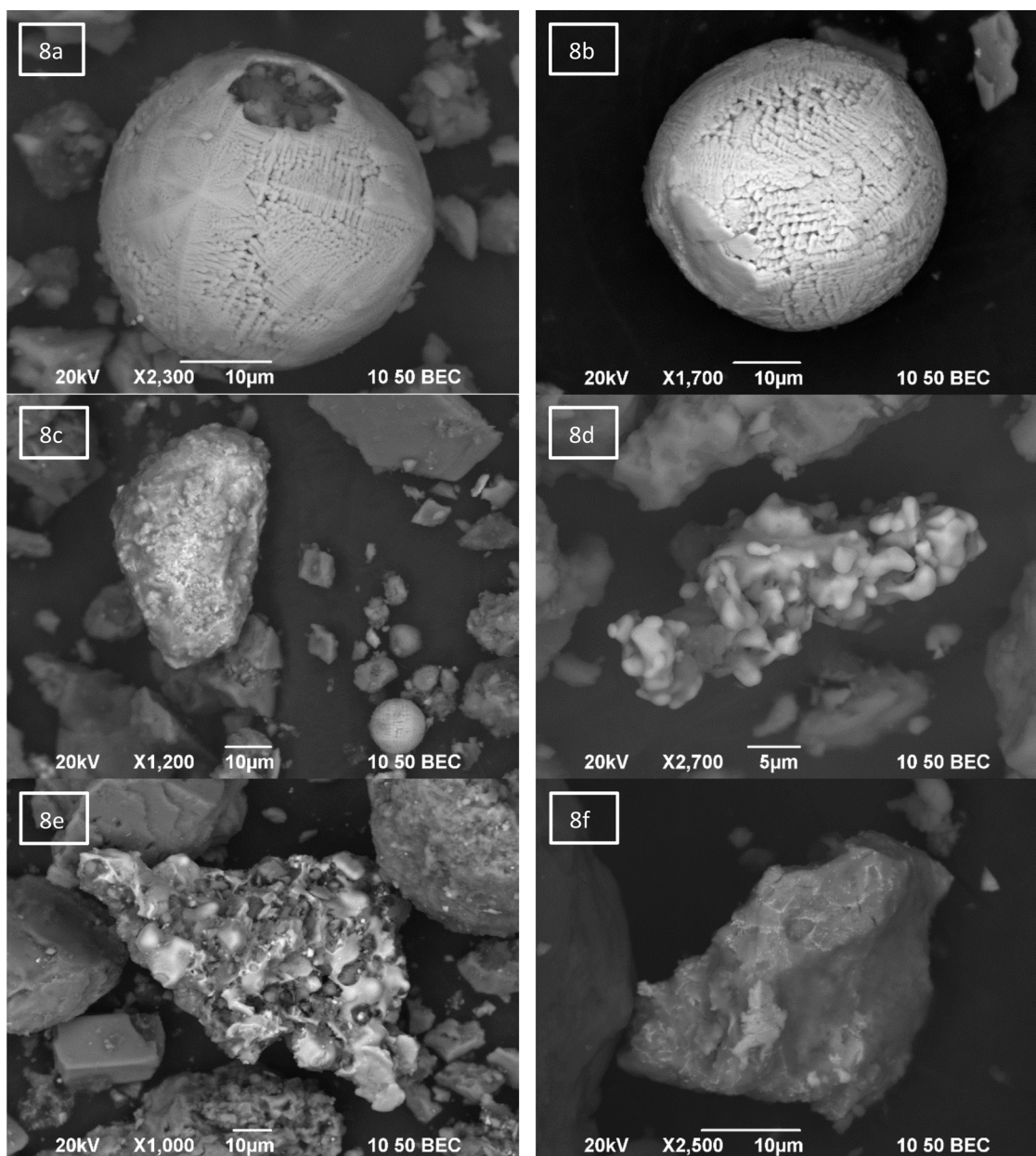
Fig. 8. SEM images of characteristic Cr, Mo, Ni and W carrier particles. Micrographs were made in BSE mode.

environments is also a consequence of brake pads wear.

Strong enrichments of Bi, Mo and Pt detected in urban areas could also be explained by emissions from traffic, since Bi is used as catalyst in rubber production and as a substitute for Pb in alloys and solders (Kabata-Pendias, 2011). Molybdenum can be emitted from diesel engines (Wang et al., 2003) while Pt is characteristic for catalytic converter attrition (Prichard et al., 2009). Silver enrichment could be a result of the release of Ag particles from antibacterial and antifungal agents from facades and paints (Kaegi et al., 2010).

Spherical particles, metal shavings and MMVF were another characteristic anthropogenically derived particles identified by SEM/EDS in urban SD. They significantly differ from natural particles in morphology as well as in elemental composition. Their abundancy can reveal prevailing types of anthropogenic effects, like combustion emissions or mechanical abrasion, producing silicate, Fe-O and Ca-ferrite soot spheres and elongated metal shavings respectively. Identified MMVF could also be a product of deterioration of various construction materials, especially insulation products that contain mineral wool or degradation of historical roofing and building materials which include asbestos (Salonen et al., 2009).

SD in this study showed exceptionally high enrichments of Ca, Mg and Sr compared to their levels in soil. This finding is also in-line with the findings of Žibret (2018). Deterioration of construction materials, such as pavements, aggregates, mortar, lime and similar, which usually contains high levels of Ca and Mg, could explain the above-mentioned phenomenon.

Comparison of Cr, Cu, Mo, Ni, Sb and Sn levels in SD with the results from other similar areas (Table 2) show that corresponding Slovenian urban median levels are generally lower, compared to densely populated and industry-intensive areas, such as Baoji, Düzce, Urumqi or Tianjin and higher, compared to predominantly residential urban areas, such as Luanda and Ottawa. These findings apply regardless of the fraction analyzed and analytical technique used. SD levels for Ni and especially for Cr from Witbank town, where large steel mills are located, exceed most of the values recorded in Slovenia.

SD composition, beside natural sources, is influenced by metallurgical industry emissions and urbanization processes, where traffic, fuels combustion, and weathering of construction materials can be

Table 2

Comparison of urban SD elemental levels with other studies of SD in urban environments. Elemental levels are in mg/kg.

City		Fraction	Method	Digestion	Cu	Cr	Mo	Ni	Sb	Sn	Reference
Slovenia (urban env.)	median	< 63 μm	ICP-MS	aqua regia	75	45	3.1	24	3	16	This study
Luanda, Angola	median	< 100 μm	ICP-MS	aqua regia	39	26	1.9	9.7	2.8	–	Ferreira-Baptista and De Miguel (2005)
Ottawa, Canada	median	100–250 μm	ICP-MS	HNO$_3$-HF	29.54	41.8	1.38	14.6	0.42	1.19	Rasmussen et al. (2001)
Baoji, China	average	< 75 μm	XRF	–	123.2	126.7	–	48.8	–	–	Lu et al. (2010)
Tianjin, China	average	< 75 μm	ICP-MS	HF-HCl-HNO$_3$	527.54	–	12.82	77.88	21.81	82.87	Zhang et al. (2019)
Urumqi, China	average	< 149 μm	ICP-MS	HNO$_3$-H$_2$-SO$_4$-HF	94.54	54.28	–	43.28	–	–	Wei et al. (2009)
Witbank, South Africa	median	< 125 μm	ICP-MS	Four acid	58.4	3,050	2.45	53.0	1.50	4.40	Žibret et al. (2013)
Düzce, Turkey	average	< 125 μm	ICP-MS	HNO$_3$-HClO$_4$-HF	99	122	28	31	28	39	Taşpınar and Bozkurt (2018)

recognized as the most traceable particle sources. Possible reduction of emissions from steel mills and similar industries could be achieved by more effective dust control (Žibret, 2012), while decreasing influence of traffic related emissions might be possible with relevant landscape planning of urban surfaces and promotion of alternative means of transportation.

This study will be further upgraded by using SEM/EDS which, combined with statistical analysis on the particle level, could provide additional support to the claims presented in this study. It will also try to quantitatively determine the impact of soil resuspension to SD composition, which has not been evaluated in this study. Findings from this research can be utilized for future studies of SD composition at other known contaminated areas, where historical industrial activities and recent emissions both contribute to the presence of PTEs in SD. Further studies could also be done to determine health impact of SD to humans and plants (Aricak et al., 2019). Another suggested in-vitro study could be to investigate how specific particles change when exposed to body fluids, especially to those in digestive tract or lungs. Nevertheless, the results of this study will provide further solid and relevant scientific information towards establishing SD as a reliable marker of anthropogenic dust emissions and can serve as a solid knowledge-base for better future landscape planning and management, which will hopefully result in creating cleaner, healthier and more sustainable urban environments.

5. Conclusions

Street dust was sampled in nation-wide sampling campaign. Chemical analysis of < 0.063 mm fraction and SEM/EDS analysis of individual particles revealed several anthropogenic sources of PTEs. Comparison of elemental composition between urban and countryside environments shows that Sn, Cu, Sb, Bi, Ag, Mo, Pt, Pb, Cr, Zn, W and Ni are significantly enriched in SD in urban environments. SEM/EDS inspection of urban SD identified organic thread-like particles, probably generated during tire wear, and irregular, tile-like shaped particles with diameter bellow 20 μm, probably generated during mechanical abrasion of brake pads, as the most common carriers of Ba, Cu, Sn and Zn.

Another important source of particles accumulated in SD in the study area is steel production and processing. Strong anomalies of Cr, Mo, Ni and W were recognized around active steel mills. Hollow spherical particles and irregular particles either with relatively plain surface or bubble-shaped protuberances and cavities were identified in proximity of steel plants as the main carriers of Cr, Mo, Ni and W. Such kinds of particles were not found in other urban areas. Elemental levels of Cr, Mo, Ni and W show strong distance dependency, they decrease exponentially with increasing distance from the steel mill and reach regional urban background at a distance between 15 and 20 km.

Acknowledgements

Appendix A. Supplementary data

Supplementary material related to this article can be found, in the online version, at doi:https://doi.org/10.1016/j.jhazmat.2019.120963.

References

Aricak, B., Cetin, M., Erdem, R., Sevik, H., Cometen, H., 2019. The change of some heavy metal concentrations in scotch pine (Pinus sylvestris) depending on traffic density, organelle and washing. Appl. Ecol. Environ. Res. 17 (3), 6723–6734. https://doi.org/10.15666/aeer/1703_67236734.

Barbieri, M., 2016. The importance of Enrichment Factor (EF) and Geoaccumulation Index (Igeo) to evaluate the soil contamination. J. Geol. Geophys. 5 (1). https://doi.org/10.4172/2381-8719.1000237.

Boscolo, M., Padoano, E., 2011. Monitoring of particulate emissions to assess the outcomes of retrofitting measures at an ironmaking plant. ISIJ Int. 51, 1553–1560. https://doi.org/10.2355/isijinternational.51.1553.

Cetin, M., Sevik, H., 2016. Change of air quality in Kastamonu city in terms of particulate matter and CO2 amount. Oxid. Commun. 39 (4–II), 3394–3401.

Ferreira-Baptista, L., De Miguel, E., 2005. Geochemistry and risk assessment of street dust in Luanda, Angola: a tropical urban environment. Atmos. Environ. 39 (25), 4501–4512. https://doi.org/10.1016/j.atmosenv.2005.03.026.

Gaberšek, M., Gosar, M., 2018. Geochemistry of urban soil in the industrial town of Maribor, Slovenia. J. Geochem. Explor. 187, 141–154. https://doi.org/10.1016/j.gexplo.2017.06.001.

Gosar, M., Šajn, R., Bavec, Š., Gaberšek, M., Pezdir, V., Miler, M., 2019. Geochemical background and threshold for 47 chemical elements in Slovenian topsoil layer. Geologija 62 (1). https://doi.org/10.5474/geologija.2019.001.

Grigoratos, T., Martini, G., 2015. Brake wear particle emissions: a review. Environ. Sci. Pollut. Res. 22, 2491–2504. https://doi.org/10.1007/s11356-014-3696-8.

Gunawardana, C., Goonetilleke, A., Egodawatta, P., Dawes, L., Kokot, S., 2012. Source characterisation of road dust based on chemical and mineralogical composition. Chemosphere 87 (2), 163–170. https://doi.org/10.1016/j.chemosphere.2011.12.012.

Hama, S.M.L., Cordell, R.L., Staelens, J., Mooibroek, D., Monks, P.S., 2018. Chemical composition and source identification of PM10 in five North Western European cities. Atmos. Res. 214, 135–149. https://doi.org/10.1016/j.atmosres.2018.07.014.

Kabata-Pendias, A., 2011. Trace Elements in Soils and Plants, 4th ed. CRC Press, Boca Raton, Fla.

Kaegi, R., Sinnet, B., Zuleeg, S., Hagendorfer, H., Mueller, E., Vonbank, R., Boller, M., Burkhardt, M., 2010. Release of silver nanoparticles from outdoor facades. Environ. Pollut. 158 (9), 2900–2905. https://doi.org/10.1016/j.envpol.2010.06.009.

Kukutschová, J., Moravec, P., Tomášek, V., Matějka, V., Smolík, J., Schwarz, J., Seidlerová, J., Šafářová, K., Filip, P., 2011. On airborne nano/micro-sized wear particles released from low-metallic automotive brakes. Environ. Pollut. 159 (4), 998–1006. https://doi.org/10.1016/j.envpol.2010.11.036.

Ledoux, F., Kfoury, A., Delmaire, G., Roussel, G., El Zein, A., Courcot, D., 2017. Contributions of local and regional anthropogenic sources of metals in PM 2.5 at an urban site in northern France. Chemosphere 181, 713–724. https://doi.org/10.1016/j.chemosphere.2017.04.128.

Lu, X., Wang, L., Li, L.Y., Lei, K., Huang, L., Kang, D., 2010. Multivariate statistical analysis of heavy metals in street dust of Baoji, NW China. J. Hazard. Mater. 173 (1–3), 744–749. https://doi.org/10.1016/j.jhazmat.2009.09.001.

Mbengue, S., Alleman, L.Y., Flament, P., 2015. Bioaccessibility of trace elements in fine and ultrafine atmospheric particles in an industrial environment. Environ. Geochem. Health 37 (5), 875–889. https://doi.org/10.1007/s10653-015-9756-2.

McQueen, A.D., Johnson, B.M., Rodgers, J.H., English, W.R., 2010. Campus parking lot stormwater runoff: physicochemical analyses and toxicity tests using Ceriodaphnia dubia and Pimephales promelas. Chemosphere 79 (5), 561–569. https://doi.org/10.1016/j.chemosphere.2010.02.004.

Miler, M., Gosar, M., 2013. Assessment of metal pollution sources by SEM/EDS analysis of

solid particles in snow: a case study of žerjav, Slovenia. Microsc. Microanal. 19 (6), 1606–1619. https://doi.org/10.1017/S1431927613013202.

Miler, M., Gosar, M., 2015. Chemical and morphological characteristics of solid metal-bearing phases deposited in snow and stream sediment as indicators of their origin. Environ. Sci. Pollut. Res. 22 (3), 1906–1918. https://doi.org/10.1007/s11356-014-3589-x.

Miler, M., Gosar, M., 2019. Assessment of contribution of metal pollution sources to attic and household dust in Pb-polluted area. Indoor Air 29 (3), 487–498. https://doi.org/10.1111/ina.12548.

Padoan, E., Amato, F., 2018. Vehicle non-exhaust emissions: impact on air quality. Non-Exhaust Emissions. Elsevier, pp. 21–65. https://doi.org/10.1016/B978-0-12-811770-5.00002-9.

Pant, P., Baker, S.J., Shukla, A., Maikawa, C., Godri Pollitt, K.J., Harrison, R.M., 2015. The PM 10 fraction of road dust in the UK and India: characterization, source profiles and oxidative potential. Sci. Total Environ. 530–531, 445–452. https://doi.org/10.1016/j.scitotenv.2015.05.084.

Powell, J.W.D., Hunt, A., Abraham, J.L., 2002. Anthropogenic vanadium-chromium-iron and cerium-lanthanum-iron particles in settled urban house dust: CCSEM identification and analysis. Water Air Soil Pollut. 135 (1), 207–217.

Prichard, H.M., Sampson, J., Jackson, M., 2009. A further discussion of the factors controlling the distribution of Pt, Pd, Rh and Au in road dust, gullies, road sweeper and gully flusher sediment in the city of Sheffield, UK. Sci. Total Environ. 407 (5), 1715–1725. https://doi.org/10.1016/j.scitotenv.2008.10.042.

Rasmussen, P.E., Subramanian, K.S., Jessiman, B.J., 2001. A multi-element profile of house dust in relation to exterior dust and soils in the city of Ottawa, Canada. Sci. Total Environ. 267 (1), 125–140.

Salonen, H.J., Lappalainen, S.K., Riuttala, H.M., Tossavainen, A.P., Pasanen, P.O., Reijula, K.E., 2009. Man-made vitreous fibers in office buildings in the Helsinki Area. J. Occup. Environ. Hyg. 6 (10), 624–631. https://doi.org/10.1080/15459620903133667.

Sevik, H., Ozel, H.B., Cetin, M., Özel, H.U., Erdem, T., 2019. Determination of changes in heavy metal accumulation depending on plant species, plant organism, and traffic density in some landscape plants. Air Qual. Atmos. Health 12 (2), 189–195. https://doi.org/10.1007/s11869-018-0641-x.

Sylvestre, A., Mizzi, A., Mathiot, S., Masson, F., Jaffrezo, J.L., Dron, J., Mesbah, B., Wortham, H., Marchand, N., 2017. Comprehensive chemical characterization of industrial PM 2.5 from steel industry activities. Atmos. Environ. 152, 180–190. https://doi.org/10.1016/j.atmosenv.2016.12.032.

Šajn, R., 1998. Geochemical soil survey at Jesenice area, Slovenia. Geologija 41, 319–338. https://doi.org/10.5474/geologija.1998.016.

Šajn, R., 2006. Factor analysis of soil and attic-dust to separate mining and metallurgy

influence, Meza Valley, Slovenia. Math. Geol. 38 (6), 735–747. https://doi.org/10.1007/s11004-006-9039-7.

Taşpınar, F., Bozkurt, Z., 2018. Heavy metal pollution and health risk assessment of road dust on selected highways in Düzce, Turkey. Environ. Forensics 19 (4), 298–314. https://doi.org/10.1080/15275922.2018.1519736.

Thorpe, A., Harrison, R.M., 2008. Sources and properties of non-exhaust particulate matter from road traffic: a review. Sci. Total Environ. 400 (1–3), 270–282. https://doi.org/10.1016/j.scitotenv.2008.06.007.

Tian, Z., Kaminski, U., Sauer, J., Maschowski, C., Stille, P., Cen, K., Gieré, R., Sommer, F., Dietze, V., Baum, A., 2017. Coarse-particle passive-sampler measurements and single-particle analysis by transmitted light microscopy at highly frequented motorways. Aerosol Air Qual. Res. 17 (8), 1939–1953. https://doi.org/10.4209/aaqr.2017.02.0064.

Turkyilmaz, A., Sevik, H., Cetin, M., Saleh, E., 2018. Changes in heavy metal accumulation depending on traffic density in some landscape plants. Pol. J. Environ. Stud. 27 (5), 2277–2284. https://doi.org/10.15244/pjoes/78620.

Wang, Y.-F., Huang, K.-L., Li, C.-T., Mi, H.-H., Luo, J.-H., Tsai, P.-J., 2003. Emissions of fuel metals content from a diesel vehicle engine. Atmos. Environ. 37 (33), 4637–4643. https://doi.org/10.1016/j.atmosenv.2003.07.007.

Wei, B., Jiang, F., Li, X., Mu, S., 2009. Spatial distribution and contamination assessment of heavy metals in urban road dusts from Urumqi, NW China. Microchem. J. 93 (2), 147–152. https://doi.org/10.1016/j.microc.2009.06.001.

Xie, R.K., Seip, H.M., Liu, L., Zhang, D.S., 2009. Characterization of individual airborne particles in Taiyuan City, China. Air Qual. Atmos. Health 2 (3), 123–131. https://doi.org/10.1007/s11869-009-0039-x.

Zhang, J., Wu, L., Zhang, Y., Li, F., Fang, X., Mao, H., 2019. Elemental composition and risk assessment of heavy metals in the PM10 fractions of road dust and roadside soil. Particuology 44, 146–152. https://doi.org/10.1016/j.partic.2018.09.003.

Zupančič, N., Turniški, R., Miler, M., Grčman, H., 2018. Geochemical fingerprint of insoluble material in soil on different limestone formations. CATENA 170, 10–24. https://doi.org/10.1016/j.catena.2018.05.040.

Žibret, G., 2012. Impact of dust filter installation in ironworks and construction on brownfield area on the toxic metal concentration in street dust (Celje, Slovenia). AMBIO 41 (3), 292–301. https://doi.org/10.1007/s13280-011-0188-7.

Žibret, G., 2018. Influences of coal mines, metallurgical plants, urbanization and lithology on the elemental composition of street dust. Environ. Geochem. Health. https://doi.org/10.1007/s10653-018-0228-3.

Žibret, G., Van Tonder, D., Žibret, L., 2013. Metal content in street dust as a reflection of atmospheric dust emissions from coal power plants, metal smelters, and traffic. Environ. Sci. Pollut. Res.Int. 20 (7), 4455–4468. https://doi.org/10.1007/s11356-012-1398-7.